European Journal of Radiology 165 (2023) 110925

Contents lists available at ScienceDirect

European Journal of Radiology

journal homepage: www.elsevier.com/locate/ejrad

Dynamic contrast-enhanced MRI to characterize angiogenesis in primary epithelial ovarian cancer: An exploratory study

Auni Lindgren [a,b,*], Maarit Anttila [a,b], Otso Arponen [c,d], Kirsi Hämäläinen [e,f], Mervi Könönen [c,g], Ritva Vanninen [c,h,i], Hanna Sallinen [a]

[a] Department of Obstetrics and Gynaecology, Kuopio University Hospital, Kuopio, Finland
[b] University of Eastern Finland, Faculty of Health Sciences, School of Medicine, Institute of Clinical Medicine, Obstetrics and Gynaecology, Kuopio, Finland
[c] Department of Clinical Radiology, Kuopio University Hospital, Kuopio, Finland
[d] Faculty of Medicine and Health Technology, University of Tampere, Tampere, Finland
[e] Department of Pathology and Forensic Medicine, Kuopio University Hospital, Kuopio, Finland
[f] University of Eastern Finland, Faculty of Health Sciences, School of Medicine, Institute of Clinical Medicine, Pathology and Forensic Medicine, Kuopio, Finland
[g] Department of Clinical Neurophysiology, Kuopio University Hospital, Kuopio, Finland
[h] University of Eastern Finland, Faculty of Health Sciences, School of Medicine, Institute of Clinical Medicine, Clinical Radiology, Kuopio, Finland
[i] Cancer Center of Eastern Finland, University of Eastern Finland, Kuopio, Finland

ARTICLE INFO

Keywords:
Epithelial Ovarian cancer
Magnetic Resonance Imaging
Dynamic Contrast-Enhanced MRI
Vascular Endothelial Growth Factor A
Microvessels
Angiogenesis

ABSTRACT

Purpose: Angiogenesis is essential for tumor growth. Currently, there are no established imaging biomarkers to show angiogenesis in tumor tissue. The aim of this prospective study was to evaluate whether semiquantitative and pharmacokinetic DCE-MRI perfusion parameters could be used to assess angiogenesis in epithelial ovarian cancer (EOC).

Method: We enrolled 38 patients with primary EOC treated in 2011–2014. DCE-MRI was performed with a 3.0 T imaging system before the surgical treatment. Two different sizes of ROI were used to evaluate semiquantitative and pharmacokinetic DCE perfusion parameters: a large ROI (L-ROI) covering the whole primary lesion on one plane and a small ROI (S-ROI) covering a small solid, highly enhancing focus. Tissue samples from tumors were collected during the surgery. Immunohistochemistry was used to measure the expression of vascular endothelial growth factor (VEGF), its receptors (VEGFRs) and to analyse microvascular density (MVD) and the number of microvessels.

Results: VEGF expression correlated inversely with K^{trans} (L-ROI, r = -0.395 (p = 0.009), S-ROI, r = -0.390, (p = 0.010)), V_e (L-ROI, r = -0.395 (p = 0.009), S-ROI, r = -0.412 (p = 0.006)) and V_p (L-ROI, r = -0.388 (p = 0.011), S-ROI, r = -0.339 (p = 0.028)) values in EOC. Higher VEGFR-2 correlated with lower DCE parameters K^{trans} (L-ROI, r = -0.311 (p = 0.040), S-ROI, r = -0.337 (p = 0.025)) and V_e (L-ROI, r = -0.305 (p = 0.044), S-ROI, r = -0.355 (p = 0.018)). We also found that MVD and the number of microvessels correlated positively with AUC, Peak and WashIn values.

Conclusions: We observed that several DCE-MRI parameters correlated with VEGF and VEGFR-2 expression and MVD. Thus, both semiquantitative and pharmacokinetic perfusion parameters of DCE-MRI represent promising tools for the assessment of angiogenesis in EOC.

Abbreviations: VEGF, vascular endothelial growth factor; VEGFR, vascular endothelial growth factor receptor; MVD, microvascular density; EES, extravascular, extracellular space volume; K^{trans}, a rate constant for transfer of contrast agent from plasma to EES; K_{ep}, rate constant for transfer of contrast agent from EES to plasma; V_e, contrast agent distribution volume, EES volume fraction; V_p, plasma volume fraction; AUC, area under the enhancement curve; WashIn, initial up-slope of the DCE curve; WashOut, initial down-slope of the DCE curve; Peak, peak/maximal enhancement; Time To Peak, time when contrast agent reaches the peak volume; AIF, arterial input function.

* Corresponding author at: Department of Gynecology and Obstetrics, Kuopio University Hospital, P.O. Box 100, Kuopio FIN-70029, KYS, Finland.
E-mail address: auni.lindgren@pshyvinvointialue.fi (A. Lindgren).

https://doi.org/10.1016/j.ejrad.2023.110925
Received 6 January 2023; Received in revised form 2 May 2023; Accepted 9 June 2023
Available online 11 June 2023
0720-048X/© 2023 The Authors. Published by Elsevier B.V. This is an open access article under the CC BY license (http://creativecommons.org/licenses/by/4.0/).

1. Introduction

Epithelial ovarian cancer (EOC) is one of the most lethal gynecological malignancies. It is frequently diagnosed only when it has spread extensively, because there may not be early symptoms; therefore, the prognosis of EOC remains poor [1]. Angiogenesis is essential for both tumor growth and metastasis and many angiogenic growth factors and their receptors promote and regulate angiogenesis in tumor progression. Recently, new biological agents targeting angiogenesis of cancer have been approved in the therapy of several cancers, including EOC. The most extensively studied angiogenic growth factor has been the vascular endothelial growth factor (VEGF) family [2] with seven different subtypes (VEGF-A, -B, -C, -D, -E, -F and placental growth factor PlGF) being described [3]. These factors signal through three tyrosine kinase receptors VEGFR-1 (Flt-1), VEGFR-2 (KDR/Flt-1) and VEGFR-3 (Flt-4) [2]. The major receptors involved in angiogenesis, vasculogenesis and vascular permeability are VEGFR-1 and −2, with VEGF-A and -B mainly acting through these two tyrosine kinase receptors [4]. VEGFR-3 appears to be the most important receptor promoting lymph angiogenesis with VEGF-C and -D most often binding to this receptor [5,6]. Cross signaling between different ligands and receptors also occurs [7,8]. Bevacizumab is the most widely investigated and clinically used anti-angiogenic agent; this compound is a recombinant humanized monoclonal antibody targeting VEGF [9].

Since new targeted therapies are under development with some of them are already being administered in the clinical use, it is crucial to develop biomarkers to identify and follow-up patients who might benefit from these specific treatments while minimizing unnecessary toxicity and costs [10,11]. Currently, there are no reliable indicators that could predict the response to antiangiogenic treatments.

In clinical situations, the Response Evaluation Criteria In Solid Tumor (RECIST) are frequently used in evaluating the response of solid tumors to treatment. However, antiangiogenic agents may cause tumoral necrosis and apoptosis without changes in the tumor's volume [12]. In addition to conventional magnetic resonance imaging (MRI) protocols diffusion weighted imaging (DWI) and dynamic contrast enhanced (DCE) sequences have been studied in the risk stratification and prognosis of ovarian cancer. DWI associates with tumor cellularity, macromolecule structures and viscosity rather than with angiogenesis. DCE sequences provide information about vascular permeability and perfusion [13–15]. Semiquantitative and perfusion DCE parameters have been shown to be able to differentiate benign from malignant tumors [16–18], serve as predictive biomarkers [19,20] and enable a response evaluation [21,22]. Therefore, we hypothesized that DCE-MRI could also reveal important information of tumor angiogenesis in EOC.

This is the first study where the angiogenic properties, including those of the growth factor VEGF and its receptor and microvascular density (MVD) have been extensively correlated with different DCE parameters. The aim of this prospective study was to evaluate whether DCE semiquantitative and pharmacokinetic perfusion parameters could be used to assess angiogenesis in epithelial ovarian cancer.

2. Materials and methods

2.1. Patients and study design

A total of 38 patients (median age 65 years, range 47–86 years) diagnosed with epithelial ovarian cancer in Kuopio University Hospital between 2011 and 2014 were included in this prospective study. The study protocol was approved by the Local Research Ethical Committee (number 5302473). We obtained written informed consents from all study subjects. The eligibility criteria were as follows: 1) diagnosis of primary EOC (including fallopian tube cancer or primary peritoneal carcinoma as they are all treated as one entity), 2) measurable disease in the diagnostic computed tomography (CT) and 3) possibility to perform MR imaging with 3.0 T scanner. The exclusion criteria were contraindications to gadolinium contrast agent, pacemaker or other metal foreign object not compliable to MRI imaging or too poor general health preventing supine position. Staging was based on the standards of the International Federation of Gynecology and Obstetrics (FIGO). The World Health Organization (WHO) criteria were used to determine the histological type. Preoperative diagnostic 3.0 T MRI with a structured protocol was performed for all the recruited patients before any treatment. A multidisciplinary team scheduled neoadjuvant chemotherapy for five patients; these patients were excluded from immunohistopathological analyses. In order to measure expression of VEGF, its receptors and properties of microvessels, tumor samples were harvested at the time of primary surgery. All patients received adjuvant treatment after surgery, one patient with stage IA disease received single carboplatin and others received combination of carboplatin and paclitaxel. The characteristics of the patients are described in Table 1.

2.2. Imaging protocol and image analysis

MRI examinations were performed with a 3.0 T scanner (Philips Achieva 3.0 T TX, Philips N.V.) and a body coil (Sense-XL-Torso), the whole abdomen was covered. The structured imaging protocol included the following sequences: 1) T2-weighted (T2W) (transaxial, sagittal and coronal, TR 651 ms, TE 80 ms, flip angle 90°, resolution 0.7 mm × 0.7 mm × 0.5 mm); 2) DUAL- fast field echo (FFE) sequence (TR 180 ms, TE 1.15 ms outphase and 2.30 ms inphase, flip angle 55°, resolution1.3 mm × 1.3 mm × 5.0 mm); 3) transaxial fat suppressed SPAIR (TR 744 ms, TE 70 ms, flip angle 90°); 4) gadolinium dynamic eThrive SENSE DCE sequence (TR 3.8 ms, TE 1.8 ms, flip angle 10°, resolution 0.9 mm × 0.9 mm × 5.0 mm, at 6.7 s intervals a total of 23 timeframes); 5) T1w post-contrast images (TR 6.9 ms, TE 3.5 ms, flip angle 10°, resolution 1.5 mm × 1.5 mm × 3.0 mm); 6) DWI ((TR 490 ms, TE 48 ms, flip angle 90°, resolution 1.81.8 mm × 1.8 mm × 5.0 mm)(b values 0, 300, 600 s/mm^2)) and 7) DWIBS (b value 800 s/mm^2) sequences. After the acquisition of the native images (image stack 1), the contrast agent (gadoterate meglumine (Dotarem 279.3 mg/ml)) was injected intravenously during the DCE sequence imaging. The contrast agent was administered as a bolus using a MRI-compatible power injector (Optistar Elite, Covidien), the dose was 0.1 mmol/kg at a rate of 4 ml/s, followed by a 20 ml

Table 1
Patient characteristics.

Characteristics	n (%)*	n (%)**
Patients	38 (100)	30 (100)
Age (years)	66, range 47–86	66, range 47–86
Ascites	29 (76)	24 (80)
No ascites	9 (24)	6 (20)
BMI > 25	21 (55)	18 (60)
BMI ≤ 25	16 (42)	12 (40)
Histological grade		
1	2 (5)	1 (3)
2	13 (34)	10 (33)
3	23 (61)	19 (64)
Stage		
I	6 (16)	5 (17)
II	2 (5)	2 (7)
III	15 (9.5)	13 (43)
IV	15 (39.5)	10 (33)
Histological type		
Serous high grade	25 (66)	20 (67)
Endometrioid	6 (16)	5 (17)
Mucinous	2 (5)	0 (0)
Clear cell	1 (3)	1 (3)
Other	4 (10)	4 (13)
Residual tumor at debulking surgery		
None	17 (45)	15 (50)
</= 1 cm	15 (40)	12 (40)
> 1 cm	5 (13)	3 (10)

Values are count (n) and percentage of subjects (%). BMI = body mass index. *All Patients, **Patients included in analyses.

flush of 0.9 % sodium chloride solution. Subsequently, image acquisition was continued (image stacks 2–23). The acquisition time was 6.7 s/stack in the perfusion scan for 51 slices and acquisition matrix 267*387.

Two observers (A.L. and O.A. with 6 and 4 years of experience in gynecological imaging, respectively) performed the semiquantitative and pharmacokinetic perfusion parameter measurements. We evaluated all MRI- and DCE- sequences blinded to the histopathological information using a Sectra PACS workstation (IDS7, Version 15.1.20.2) and performed the DCE analysis using NordicIce (version: 2.3.13, NordicNeuroLab) software. A detailed description of image analysis has been reported previously [20]. We analysed nine parameters. Five semiquantitative parameter maps were generated from the DCE curve: 1) AUC, area under the DCE curve; 2) PEAK, the amplitude of peak enhancement; 3) Time-to-Peak, the time when contrast agent reaches peak enhancement; 4) WashIn, the up-slope, the positive slope from beginning to peak enhancement and 5) WashOut, the down-slope of the curve. Motion correction was done automatically. NordicIce software generated the following perfusion parameter maps: 6) K^{trans}, that reflects the contrast agenťs flow from plasma to the extravascular extracellular space (EES); 7) K_{ep}, the opposite direction rate constant from EES to plasma; 8) V_e, reflecting contrast agent distribution volume; and 9) V_p, the fraction of contrast agent remaining in the plasma automatically using pharmacokinetic modeling of contrast kinetics according to the Tofts model. The arterial input function (AIF), for the perfusion parameters, was determined by using a small AIF ROI on the iliac artery (common or external). The AIF shape was visually inspected for all the patients. B1 maps and T1 mapping were not used because of the clinical practice at the time of the study design. When analysing DCE-MRI images, we visually determined the phase with the peak enhancement of the tumor. The ROIs were then positioned within the tumor on DCE-MRI images of the phase with the most evident lesion, without standardizing the post-contrast time point. A large ROI (L-ROI) and a small ROI (S-ROI) were drawn on the primary tumors and the contralateral ovarian tumor, if possible (Fig. 1). The L-ROI was delineated free-hand to cover the whole solid tumor area in one plane (cystic and necrotic areas were avoided) and the small circle S-ROI (size 15 × 15 pixels) was placed on the most intensively enhancing area. For tumor localization and ROI delineation all T2W-, T1W-, DWI- and contrast-enhanced T1W- images were available.

2.3. Immunohistochemistry

Tissue samples were embedded in paraffin and cut into 5 μm thick sections. Sections were processed for hematoxylin-eosin, VEGF (1:250, Santa Cruz) VEGFR-1 (1:15, Santa Cruz), VEGFR-2 (1:750, Cell Signaling), and VEGFR-3 (1:1000, Millipore/Chemicon) and CD34 (1:500, DAKO) staining. The expressions of VEGF and its receptors were evaluated from epithelial cells and the stroma microscopically (Leitz Wetzlar 512,761/20). The percentage of stained cells and the staining intensity were calculated. Fig. 2. illustrates VEGF staining. The numbers of microvessels, mean microvessel area (μm^2), total percent of microvascular area of tumors (TVA) and microvessel density (MDV) were measured from CD34-immunostained sections using analySIS software (Olympus, Soft Imaging System, GmbH) at × 200 magnification in a blinded manner. Three different fields representing maximal microvessel areas were selected from each tumor [23–26]. Necrotic areas were avoided. Five patients were excluded from the immunohistopathological analyses, because they received neoadjuvant chemotherapy which can evoke cellular damage.

2.4. Statistical analyses

SPSS 22.0 for Windows (Version 22.0, 1989–2013, SPSS Inc.) was used for all statistical analyses. Different DCE values from L-ROIs and S-ROIs were used as continuous variables in the statistical analyses. Histological parameters were graded with three (grades 1 to 3) tier grading

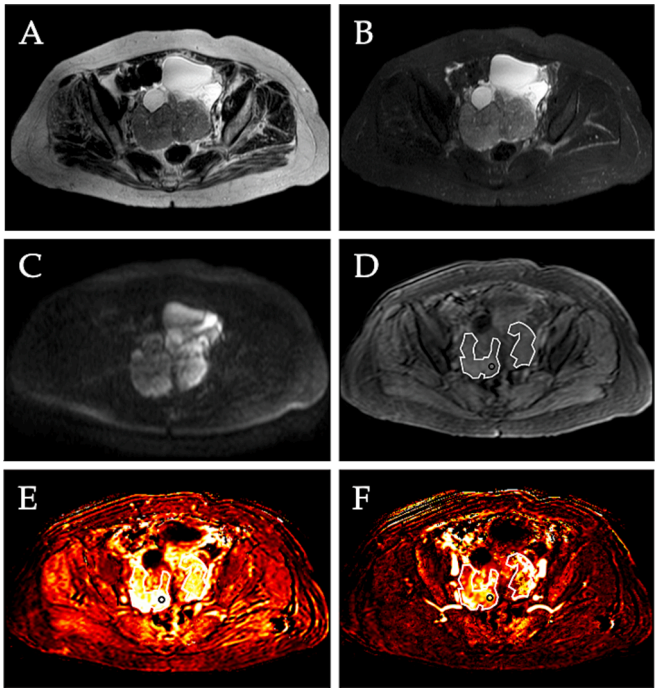

Fig. 1. A 67-year-old woman with a primary high grade serous ovarian adenocarcinoma imaged with (A) T2-weighted, (B) T2spair fat saturated, (C) DWIBS sequence (b 800), (D) in enhancement imaging, (E) with color-encoded Ktrans (a rate constant for transfer of contrast agent from plasma to extravascular extracellular space (EES)) map, and (F) Kep (a rate constant for transfer of contrast agent from EES to plasma) map. (D) illustrates the placement of the region of interest in enhancement imaging. A large ROI (L-ROI) was placed to cover the whole tumor on the slice where the tumor was largest; the contralateral tutor was also delineated whenever feasible. A small ROI (S-ROI) was placed on those subregions appearing to have the highest enhancement.

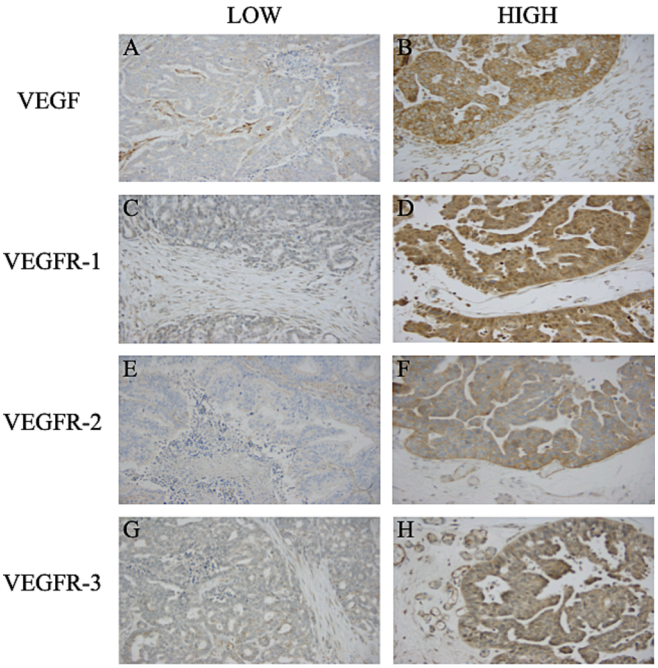

Fig. 2. Examples of ovarian tumors having low and high expressions of (A, B) VEGF, (C, D) VEGFR-1, (E, F) VEGFR-2 and (G, H) VEGFR-3 by immunohistochemistry.

system. Values are presented as mean ± SD unless otherwise stated. Interobserver correlation was tested with Interclass correlation coefficient (ICC). The Chi-square test was used to analyse frequency differences between the groups. Bivariate correlations between continued variables were analysed with the Pearson test. P values < 0.05 were regarded as statistically significant.

3. Results

A total of 38 patients were recruited; three of them had to be excluded from DCE imaging analyses due to insufficient imaging quality, and five from histopathological analysis because of neoadjuvant chemotherapy. We analysed the primary site and also the contralateral ovarian tumor when it was sufficient; some patients had no measurable contralateral ovarian tumor. There was a total of 49 lesions evaluated in these analyses. The median age of the patients was 66 years (range 47–86 years). The mean diameter of L-ROI was 77 mm (range 23–233 mm), and the set size of S-ROI was 15 × 15 pixels (from 6 to 12 mm).

The two readers reached excellent Interobserver agreement for most of the DCE parameters, AUC, Peak, Time to peak, WashIn, K^{trans}, K_{ep}, and V_e (ICC 0.951–0,994 for L-ROI and 0.928–0.991 for S-ROI). The agreement was moderate to good for WashOut (ICC 0.584 using S-ROI) and for V_p (ICC 0.637 using L-ROI and 0.614 using S-ROI).

In our cohort, VEGF correlated inversely with DCE parameters K^{trans} (L-ROI r = -0.395 (p = 0.009), S-ROI r = -0.390 (p = 0.010)), V_e (L-ROI r = -0.395 (p = 0.009), S-ROI r = -0.412 (p = 0.006)) and V_p (L-ROI r = -0.388 (p = 0.011), S-ROI r = -0.339 (p = 0.028)) in EOC. High VEGFR-2 values correlated with lower DCE parameters K^{trans} (L-ROI r = -0.311 (p = 0.040), S-ROI r = -0.337 (p = 0.025)) and V_e (L-ROI r = -0.305 (p = 0.044), S-ROI r = -0.355 (p = 0.018)). Furthermore, VEGFR-3 correlated significantly with Time-to-Peak value (L-ROI r = -0.365 (p = 0.015), S-ROI r = -0.370 (p = 0.013)).

We conducted the analysis also only in the primary lesion site. The primary site was determined by the pathologist using debulking surgery specimens. When this information was not clearly specified, the primary site was determined as the larger ovarian tumor that had radiologically more malignant features**.** The results were congruent in this smaller cohort, i.e. VEGF correlated with K^{trans}, V_e and V_p and VEGFR-2 values correlated with lower DCE parameters K^{trans}, V_e and V_p. In addition, VEGFR-3 was correlated with Time-to-Peak variable also in this smaller cohort. The results are shown in Table 2.

3.1. Correlation between CD34 analyses and DCE parameters

We analysed microvascular density (MDV), mean microvessel area (μm^2), total percent of microvascular area of tumors (TVA) and the number of microvessels using CD34 immunohistochemical staining. MVD correlated positively with AUC (L-ROI r = 0.401 (p = 0.007), S-ROI r = 0.383 (p = 0.010)), Peak (L-ROI r = 0.402 (p = 0.007), S-ROI r = 0.385 (p = 0.010)) and WashIn (L-ROI r = 0.487 (p = 0.001), S-ROI r = 0.411 (p = 0.006)) values, see Fig. 3. Furthermore, the number of microvessels correlated with the same parameters AUC (L-ROI r = 0.427 (p = 0.004), S-ROI r = 0.427 (p = 0.006)), Peak (L-ROI, r = 0.428 (p = 0.004), S-ROI r = 0.414 (p = 0.005)) and WashIn (L-ROI r = 0.504 (p = 0.001), S-ROI r = 0.424 (p = 0.005)). The mean microvessel area correlated only with WashOut (L-ROI r = 0.305 (p = 0.044), S-ROI n.s.) and TVA only with WashIn (L-ROI r = 0.310 (p = 0.043), S-ROI n.s.). The results are shown in Table 3.

4. Discussion

The key findings of the present exploratory study were that there was a significant correlation between VEGF and VEGFR-2 expression and the pharmacokinetic DCE-MRI perfusion parameters K^{trans}, V_e and V_p of the tumor. MVD and the number of microvessels were correlated with the DCE parameters AUC, Peak and WashIn.

These results indicate that there is a connection between different DCE parameters and angiogenic markers. Indeed, K^{trans} reflects the contrast agent́s flow from plasma to the interstitial space through vessel walls; V_e i.e. extravascular extracellular space volume fraction, describes the distribution volume of the contrast agent; and V_p i.e. plasma volume fraction, in turn reflects the fraction of contrast agent remaining in the plasma, represent promising tools for the assessment of angiogenesis in ovarian cancer. These findings are important as antiangiogenic treatments are already in wide use in ovarian cancer patients and new drugs are under development.

Angiogenesis is a complex cascade, being influenced by many different ligands, growth factors and transmitters, the VEGF family is one of the most widely investigated. In our cohort, there was an inverse correlation between VEGF and DCE perfusion parameters. When there was high VEGF expression then the rate constant from plasma to the interstitial space was smaller and also the plasma volume and the extravascular extracellular space volume fraction were smaller. The most likely reason might be that the angiogenic cascade had been upregulated to allow the distribution of more blood to the growing tumor and therefore VEGF expression was higher to ensure neovascularization. When blood flow is already high then there is no more need for such high expression of VEGF and its receptors. It has been shown that more hypoxic tumors express increasingly high levels of VEGF to promote angiogenesis in an attempt to ensure the tumor's blood supply and thus the delivery of oxygen and nutrients to the growing tumor [27]. A previous study by Lindgren et al. revealed an inverse association between HIF-1alpha and K^{trans} which supports this assumption [28]. Donaldson et al. found a similar correlation in their study of head and neck cancer [29]. In angiogenesis, VEGF mainly functions through the VEGFR-2 receptor. It is not surprising that VEGFR-2 correlated in the same way as VEGF with DCE parameters in our study. Mitchell et al. also found an inverse correlation between V_p and soluble VEGFR-1 and sVEGFR-2 [30]. With respect to the other two VEGF receptors studied, i.e. VEGFR-1 and VEGFR-3, only VEGFR-3 correlated significantly with Time-to-Peak value and not with the other DCE parameters. However, the most important receptor in angiogenesis is

Table 2
Immunohistologically measured VEGF and its receptors correlate with different DCE parameters. Results are from all measurements and also from the primary site solely.

	All VEGF	Primary site VEGF	All VEGFR-2	Primary site VEGFR-2	All VEGFR-3	Primary site VEGFR-3
K^{trans} L-ROI	r −0.395, 0.009	r-0.373, 0.039	r-0.311, 0.040	r −0.310, 0.084	ns.	ns.
K^{trans} S-ROI	r −0.390, 0.010	r −0.401, 0.025	r-0.337, 0.025	r-0.366, 0.040	ns.	ns.
V_e L-ROI	r −0.395, 0.009	r −0.432, 0.015	r-0.305, 0.044	ns.	ns.	ns.
V_e S-ROI	r −0.412, 0.006	r −0.460, 0.009	r-0.355, 0.018	r-0.375, 0.034	ns.	ns.
V_p L-ROI	r −0.388, 0.011	r −0.376, 0.041	ns.	r-0.353, 0.050	ns.	ns.
V_p S-ROI	r −0.339, 0.028	ns.	ns.	r −0.357, 0.049	ns.	ns.
TimetoPeak L-ROI	ns.	ns.	ns.	ns.	r-0.365, 0.015	r −0.428, 0.014
TimetoPeak S-ROI	ns.	ns.	ns.	ns.	r-0.370, 0.013	r −0.412, 0.019

L-ROI = large region of interest, S-ROI = small region of interest, VEGF = vascular epithelial growth factor, VEGFR = vascular epithelial growth factor receptor.

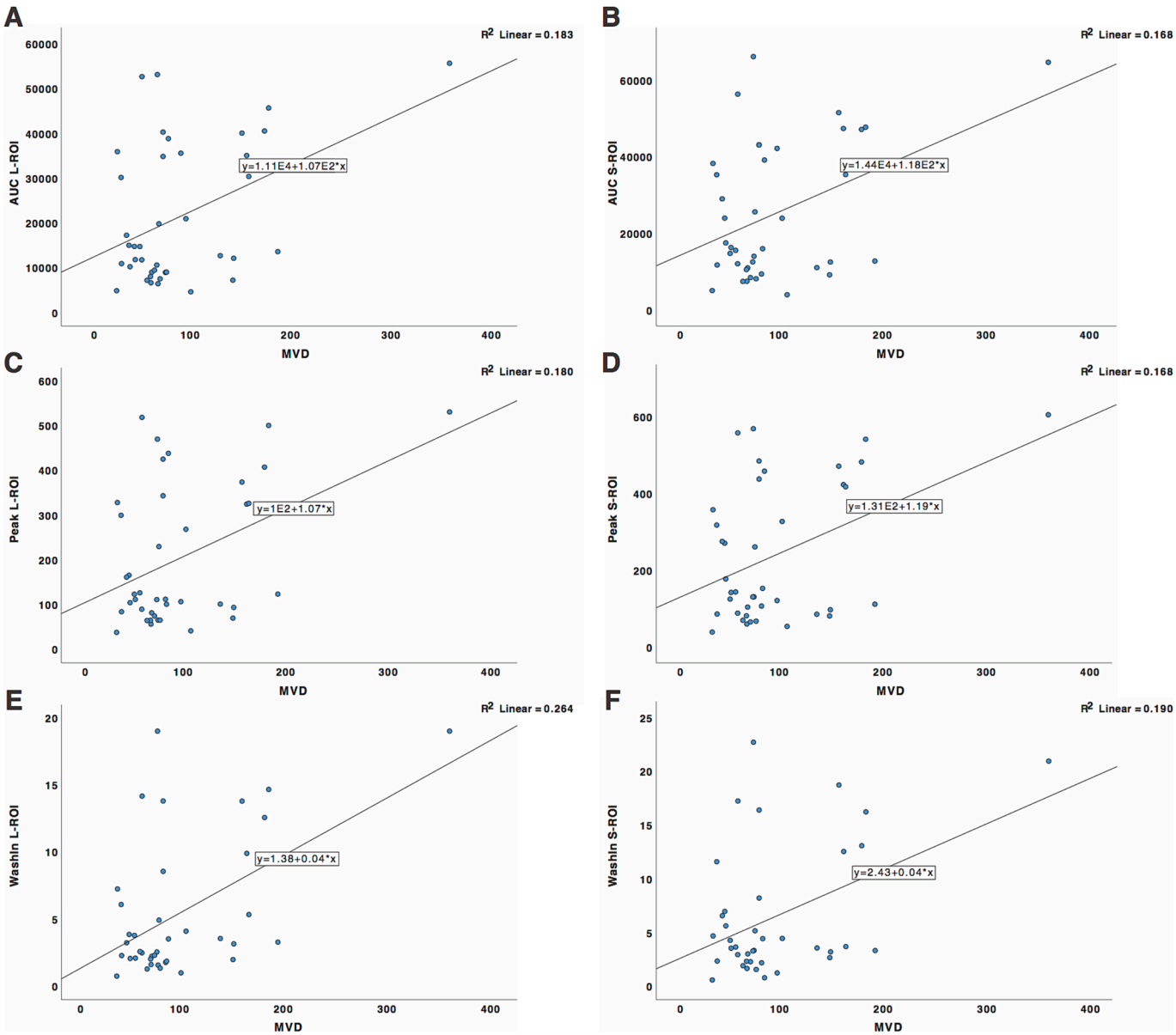

Fig. 3. The correlations between MVD and DCE parameters (A) AUC L-ROI (r = +0.401, p = 0.007), (B) AUC S-ROI (r = +0.383, p = 0.010), (C) Peak L-ROI (r = +0.404, p = 0.007), (D) Peak S-ROI (r = +0.385, p = 0.010), (E) WashIn L-ROI (r = +0.487, p = 0.001) and (F) WashIn S-ROI (r = +0.411, p = 0.006).

VEGFR-2.

The associations between DCE-MRI and angiogenic markers in different tumors have been conflicting, see Table 4 and Table 5. Some of the studies, including that reported by Donaldson et al. [29], have detected negative correlations between VEGF and DCE parameters. In some other studies, the correlation has been positive and in some other publications, there have been no significant correlations observed [31–34]. Most of these studies only identified correlations between VEGF and K^{trans} or K_{ep} but not with any other parameters [31–33]. To our knowledge, there are no publications which have as extensively examined the correlation of angiogenic markers and DCE-MRI parameters in EOC. Thomassin-Naggara et al. demonstrated that the maximal slope was correlated with a lower pericyte coverage index and stronger VEGFR-2 expression in OC. They did not observe any correlation between MVD and early enhancement patterns; VEGF expression was not reported and DCE perfusion parameters were not used [35].

In our study, MVD and the number of microvessels correlated with different DCE parameters, AUC i.e. area under enhancement curve, Peak i.e. maximal enhancement and WashIn i.e. initial up-slope of enhancement curve. It is logical that MVD and the number of microvessels correlated positively with these variables - the more vessels there are, the higher will be the enhancement and the steeper the slope. In our cohort, the pharmacokinetic DCE perfusion parameters and MVD were not significantly correlated. Yao et al., Kim et al. and Oto et al. detected positive correlations between pharmacokinetic DCE perfusion parameters and MVD in rectal, breast and prostate cancers, respectively [36–38]. Contradictory results were found in the works of Haldorsen et al., Keil et al. and Liu et al. in endometrial cancer, in meningiomas as well as in pancreatic cancer [33,34,39].

The limited number of patients in these studies could, partially, explain the differences between the outcomes (Tables 4 and 5). Furthermore, it is evident that tumors in different organs may behave differently. Fast growing EOC will need an active neoangiogenesis. In addition, differences in DCE pharmacokinetic parameter models (e.g. the Brix model and the Tofts model), scanners, scanning protocol, gradients, contrast media injection timing and ROI placement could all contribute to the conflicting results in the literature. Lastly, some investigators have used CD31, not CD34, as their immunohistochemical

Table 3
Results of the correlations between CD34 results and the different DCE parameters.

	MVD	Medium size of the vessels	Percent of vessels	Number of vessels
AUC L-ROI	r + 0.401, 0.007	ns.	ns.	r + 0.427, 0.004
AUC S-ROI	r + 0.383, 0.010	ns.	ns.	r + 0.408, 0.006
K^{trans} L-ROI	ns.	ns.	ns.	ns.
K^{trans} S-ROI	ns.	ns.	ns.	ns.
V_e L-ROI	ns.	ns.	ns.	ns.
V_e S-ROI	ns.	ns.	ns.	ns.
V_p L-ROI	ns.	ns.	ns.	ns.
V_p S-ROI	ns.	ns.	ns.	ns.
Peak L-ROI	r + 0.402, 0.007	ns.	ns.	r + 0.428, 0.004
Peak S-ROI	r + 0.385, 0.010	ns.	ns.	r + 0.414, 0.005
TimetoPeak L-ROI	ns.	ns.	ns.	ns.
TimetoPeak S-ROI	ns.	ns.	ns.	ns.
WashIn L-ROI	r + 0.487, 0.001	ns.	r + 0.310, 0.043	r + 0.504, 0.001
WashIn S-ROI	r + 0.411, 0.006	ns.	ns.	r + 0.424, 0.005
WashOut L-ROI	ns.	r + 0.305, 0.044	ns.	ns.
WashOut S-ROI	ns.	ns.	ns.	ns.

L-ROI = large region of interest, S-ROI = small region of interest, MVD = microvessel density.

stain to analyse MVD.

There are some limitations in our study. The sample size was 38 patients, and we had to exclude 8 patients (5 treated with NACT and 3 because of poor DCE imaging quality). Some mismatch is possible between the ROI placements and the locations of the histopathological samples, although the pathologist has marked the area from where the sample was taken so that the MRI of the same area could be used. It is impossible to gather stereotactic biopsies from ovarian tumors that are located deep in the pelvis. The acquisition matrix was 267*387 and the acquisition time 6.7 s/stack for 51 slices. It is possible that a shorter temporal resolution could yield more robust data. In addition, it would be very important to standardize scanning protocols and DCE analysis. Recently, Romeo et al. suggested also the standardization of the time point used for pharmacokinetic analyses. They showed that performing the measurements using the first or the second postcontrast time point images in which the lesion is first appreciable results in more reliable and comparable pharmacokinetic parameters in comparison to the use of latter time points [40]. Indeed, standardization would help to make the results published in different institutions more comparable.

In conclusion, DCE-MRI represents a new tool to evaluate angiogenic properties of ovarian cancer. In our exploratory cohort, different DCE parameters and angiogenic markers were correlated. In the future, combining imaging biomarker data with other patient characteristics could increase the power of the decision-support models, and possibly help in the selection of antiangiogenic treatment options. However, these findings need to be validated in large further trials which will hopefully improve our understanding of the use of DCE-MRI in ovarian cancer patients treated with novel methods including antiangiogenic treatments. Furthermore, future research in multicenter settings should aim to standardize these imaging parameters.

Ethics approval and consent to participate

Ethical approval has been asked from North Savo research ethical comity, number.

Availability of data and materials

The datasets used and analysed during the current study are available from the corresponding author on reasonable request.

Table 4
Earlier studies reporting correlations between VEGF, VEGFRs and different DCE parameters.

	Tumor type	N	MRI	P/R	DCE variables	Histopathological variables	VEGF correlation
Thomassin-Naggara [35] **(2008)**	Ovarian cancer	41	1.5 T Siemens	R	EA, Tmax, MS	VEGFR-2, MDV,PCI	MS correlated with lower PCI and stronger VEGFR-2, no correlation with MVD
Mitchell [30] **(2010)**	Ovarian cancer	23	1.5 T Philips	P	iAUC60, K^{trans}, V_e, V_p, PS	VEGF, sVEGFR-1, sVEGFR-2	V_p: inverse correlation with VEGFR-1 and −2; K^{trans}: positive correlation with VEGFR-1 and −2
Donaldson [29] **(2011)**	Head and neck cancer	8	1.5 T Philips	P	F_b, PS, V_e, V_b	VEGF, hypoxia	Perfusion correlated inversely with VEGF
Ma [32]**(2017)**	Gastric cancer	32	3 T Siemens	R	K^{trans}, K_{ep}, V_e	VEGF	VEGF correlated positively with K^{trans}, no other correlations
Zhang [41]**(2008)**	Rectal cancer	34	3 T GE	P	ER_{peak}, T_{peak}, $T_{first\text{-}enhance}$	VEGF, MVD	Mean T_{peak} was significantly earlier in VEGF positive group, MVD correlate inversely with T_{peak}
Di [31]**(2019)**	Glioma	47	3 T GE	P	K^{trans}, K_{ep}, V_e, V_p	VEGF	Positive correlation with K^{trans}, no correlation with K_{ep}, V_e, V_p
Keil [34]**(2018)**	Meningioma	19	3 T Philips	P	K^{trans}, K_{ep}, V_e, V_p	VEGF, MVD	No correlation between the DCE-MRI kinetic parameters and VEGF or MVD
Liu [33]**(2015)**	Pancreatic cancer	23	3 T GE	P	K^{trans}, K_{ep}, V_e, V_p, ArIT, TTP, McSIp, CER	VEGF, MVD	Ktrans had a positive correlation with VEGF, no other correlations
Jansen [42]**(2012)**	Head and neck cancer	12	1.5 T GE	P	K^{trans}, K_{ep}, V_e,	VEGF, Ki-67, CAIX, HIF-1α	K_{ep} correlated with VEGF, Ki-67 inversely with K^{trans} and V_e, no other correlations
Present study	Ovarian cancer	31	3 T Philips	P	K^{trans}, K_{ep}, V_e, V_p, Peak, T_{peak}, WashIn, WashOut	VEGF, VEGFR-1, VEGFR-2, VEGFR-3, MVD,	VEGF correlated inversely with K^{trans}, V_e and V_p

N = number of patient, MRI = magnetic resonance imaging, P = prospective, R = retrospective, VEGF, vascular epithelial growth factor, T = tesla, VEGFR = VEGF receptor, MVD = microvessel density, PCI = pericyte coverage index, EA = enhancement amplitude, Tmax = time of half rising, MS = maximal slope, K^{trans} = a rate constant for transfer of contrast agent from plasma to extravascular, extracellular space (EES); K_{ep} = rate constant for transfer of contrast agent from EES to plasma, V_e = contrast agent distribution volume, EES volume fraction, Fb = blood flow, IAUGC = integrated area under the concentration time curve, PS = permeability surface area product, V_p = plasma volume fraction, ER_{peak} = peak enhancement ratio, T_{peak} = time to peak, $T_{first\text{-}enhance}$ = first enhancement time, ArIT = the time of arrival of contrast agent, TTP = time of peaking the contrast agent, McSIp = the maximum slope of signal intensity ascent, CER = contrast enhancement ratio, CAIX = carbonic anhydrase.

Table 5
Studies assessing the correlations between MVD and DCE perfusion parameters.

	Tumor type	P/R	N	MRI	DCE variables	MVD staining	MVD correlation
Haldorsen [39] **(2014)**	Endometrial cancer	P	54	1.5 T Siemens	MVD	CD34	K^{trans} correlated inversely with MVD
Kim [43]**(2013)**	Rectal cancer	R	63	1.5 T Siemens	Ktrans, K_{ep}	CD34, VEGF	No correlation with MVD or VEGF
Kim [37]**(2016)**	Breast cancer	R	81	3 T Siemens	Ktrans, K_{ep}, V_e histogram analyses	CD34, VEGF	Ve50 positively correlated with MVD
Surov [44] **(2017)**	Head and neck cancer	R	16	1.5 T Philips	K^{trans}, K_{ep}, V_e, iAUC	CD31	Positive correlation between Kep and vessel areas
Oto [38]**(2011)**	Prostate cancer	R	73	3 T GE	K^{trans}, K_{ep}, V_e, V_p	CD34, CD31, VEGF	Kep: positive correlation with MVD, no other correlations
Keil [34]**(2018)**	Meningioma	P	19	3 T Philips	K^{trans}, K_{ep}, V_e, V_p	CD34	No correlation between the DCE-MRI kinetic parameters and MVD
Liu [33]**(2015)**	Pancreatic cancer	P	23	3 T GE	K^{trans}, K_{ep}, V_e, V_p, ArIT, TTP, McSIp, CER	CD34	No correlations between the DCE-MRI parameters and MVD were observed
Yao [36]**(2011)**	Rectal cancer	P	26	1.5 T GE	K^{trans}, K_{ep}, V_e	CD34	K^{trans} moderately correlated with MVD
Present study	Ovarian cancer	P	31	3 T	K^{trans}, K_{ep}, V_e, V_p, AUC, Peak, T_{peak}, WashIn, WashOut	CD34	MVD and the number of vessels correlated positively with AUC, Peak and WashIn values

MRI = magnetic resonance imaging, N = number of patient, P = prospective, R = retrospective, T = tesla, VEGF = vascular endothelial growth factor, VEGFR = VEGF receptor, MVD = microvessel density, PCI = pericyte coverage index, EA = enhancement amplitude, Tmax = time of half rising, MS = maximal slope, K^{trans} = a rate constant for transfer of contrast agent from plasma to extravascular, extracellular space (EES); K_{ep} = rate constant for transfer of contrast agent from EES to plasma, V_e = contrast agent distribution volume, EES volume fraction, Fb = blood flow, IAUGC = integrated area under the concentration time curve, PS = permeability surface area product, V_p = plasma volume fraction, ER_{peak} = peak enhancement ratio, T_{peak} = time to peak, $T_{first\text{-}enhance}$ = first enhancement time, ArIT = the time of arrival of contrast agent, TTP = time of peaking the contrast agent, McSIp = the maximum slope of signal intensity ascent, CER = contrast enhancement ratio, CAIX = carbonic anhydrase.

Funding

This study was supported by The Finnish Cancer Foundation, The Kuopio University Research Foundation, The Finnish Medical Foundation and Kuopio University Hospital (the VTR grant).

CRediT authorship contribution statement

Auni Lindgren: Data curation, Formal analysis, Funding acquisition, Investigation, Methodology, Writing – original draft, Resources, Visualization. **Maarit Anttila:** Conceptualization, Project administration, Resources, Supervision, Validation, Writing – review & editing, Software, Visualization. **Otso Arponen:** Data curation, Investigation, Visualization, Writing – review & editing. **Kirsi Hämäläinen:** Resources, Supervision, Validation, Writing – review & editing. **Mervi Könönen:** Conceptualization, Methodology, Project administration, Software, Validation, Visualization, Writing – review & editing. **Ritva Vanninen:** Conceptualization, Methodology, Project administration, Resources, Supervision, Validation, Visualization, Writing – review & editing, Funding acquisition. **Hanna Sallinen:** Conceptualization, Resources, Software, Supervision, Validation, Visualization, Writing – review & editing.

Declaration of Competing Interest

The authors declare that they have no known competing financial interests or personal relationships that could have appeared to influence the work reported in this paper.

Acknowledgements

We thank Antti Lindgren, Helena Kemiläinen, Eija Myöhänen and Tuomas Selander for their skillful technical assistance.

This study was supported by The Finnish Cancer Foundation, The Kuopio University Research Foundation, The Finnish Medical Foundation and Kuopio University Hospital (the VTR grant).

References

[1] L.A. Torre, B. Trabert, C.E. DeSantis, K.D. Miller, G. Samimi, C.D. Runowicz, M. M. Gaudet, A. Jemal, R.L. Siegel, Ovarian cancer statistics, 2018, CA Cancer J Clin 68 (2018) 284–296.
[2] L. Claesson-Welsh, M. Welsh, VEGFA and tumour angiogenesis, J. Intern. Med. 273 (2013) 114–127.
[3] J.-C. Chen, Y.-W. Chang, C.-C. Hong, Y.-H. Yu, J.-L. Su, The role of the VEGF-C/VEGFRs axis in tumor progression and therapy, Int. J. Mol. Sci. 14 (2012) 88–107.
[4] M. Shibuya, Differential roles of vascular endothelial growth factor receptor-1 and receptor-2 in angiogenesis, J. Biochem. Mol. Biol. 39 (2006) 469–478.
[5] V. Joukov, K. Pajusola, A. Kaipainen, D. Chilov, I. Lahtinen, E. Kukk, O. Saksela, N. Kalkkinen, K. Alitalo, A novel vascular endothelial growth factor, VEGF-C, is a ligand for the Flt4 (VEGFR-3) and KDR (VEGFR-2) receptor tyrosine kinases, EMBO J. 15 (1996) 290–298.
[6] M.G. Achen, M. Jeltsch, E. Kukk, T. Mäkinen, A. Vitali, A.F. Wilks, K. Alitalo, S. A. Stacker, Vascular endothelial growth factor D (VEGF-D) is a ligand for the tyrosine kinases VEGF receptor 2 (Flk1) and VEGF receptor 3 (Flt4), Proc. Natl. Acad. Sci. U S A 95 (1998) 548–553.
[7] N. Nishida, H. Yano, K. Komai, T. Nishida, T. Kamura, M. Kojiro, Vascular endothelial growth factor C and vascular endothelial growth factor receptor 2 are related closely to the prognosis of patients with ovarian carcinoma, Cancer 101 (2004) 1364–1374.
[8] A. Horowitz, H.R. Seerapu, Regulation of VEGF signaling by membrane traffic, Cell. Signal. 24 (2012) 1810–1820.
[9] N. Ferrara, K.J. Hillan, H.-P. Gerber, W. Novotny, Discovery and development of bevacizumab, an anti-VEGF antibody for treating cancer, Nat. Rev. Drug. Discov. 3 (2004) 391–400.
[10] A. Gadducci, N. Lanfredini, C. Sergiampietri, Antiangiogenic agents in gynecological cancer: State of art and perspectives of clinical research, Crit. Rev. Oncol. Hematol. 96 (2015) 113–128.
[11] T.A. Yap, C.P. Carden, S.B. Kaye, Beyond chemotherapy: targeted therapies in ovarian cancer, Nat. Rev. Cancer 9 (2009) 167–181.
[12] I.M.E. Desar, C.M.L. van Herpen, H.W.M. van Laarhoven, J.O. Barentsz, W.J. G. Oyen, W.T.A. van der Graaf, Beyond RECIST: molecular and functional imaging techniques for evaluation of response to targeted therapy, Cancer Treat. Rev. 35 (2009) 309–321.
[13] P.S. Tofts, B. Berkowitz, M.D. Schnall, Quantitative analysis of dynamic Gd-DTPA enhancement in breast tumors using a permeability model, Magn. Reson. Med. 33 (1995) 564–568.
[14] I. Thomassin-Naggara, N. Soualhi, D. Balvay, E. Darai, C.-A. Cuenod, Quantifying tumor vascular heterogeneity with DCE-MRI in complex adnexal masses: a preliminary study, J. Magn. Reson. Imaging 46 (2017) 1776–1785.
[15] C.A. Cuenod, D. Balvay, Perfusion and vascular permeability: basic concepts and measurement in DCE-CT and DCE-MRI, Diagn. Interv. Imaging 94 (2013) 1187–1204.
[16] H.-M. Li, F. Feng, J.-W. Qiang, G.-F. Zhang, S.-H. Zhao, F.-H. Ma, Y.-A. Li, W.-Y. Gu, Quantitative dynamic contrast-enhanced MR imaging for differentiating benign, borderline, and malignant ovarian tumors, Abdom. Radiol. 43 (2018) 3132–3141.

[17] I. Thomassin-Naggara, N. Soualhi, D. Balvay, E. Darai, C.A. Cuenod, Quantitative dynamic contrast-enhanced MR imaging analysis of complex adnexal masses: a preliminary study, Eur. Radiol. 22 (2012) 738–745.
[18] E. Sala, A. Rockall, D. Rangarajan, R.A. Kubik-Huch, The role of dynamic contrast-enhanced and diffusion weighted magnetic resonance imaging in the female pelvis, Eur. J. Radiol. 76 (2010) 367–385.
[19] B.R. Dickie, C.J. Rose, L.E. Kershaw, S.B. Withey, B.M. Carrington, S.E. Davidson, G. Hutchison, C.M.L. West, The prognostic value of dynamic contrast-enhanced MRI contrast agent transfer constant Ktrans in cervical cancer is explained by plasma flow rather than vessel permeability, Br. J. Cancer 116 (2017) 1436–1443.
[20] A. Lindgren, M. Anttila, O. Arponen, S. Rautiainen, M. Könönen, R. Vanninen, H. Sallinen, Prognostic value of preoperative dynamic contrast-enhanced magnetic resonance imaging in epithelial ovarian cancer, Eur. J. Radiol. 115 (2019) 66–73.
[21] M.A. Zahra, K.G. Hollingsworth, E. Sala, D.J. Lomas, L.T. Tan, Dynamic contrast-enhanced MRI as a predictor of tumour response to radiotherapy, LancetOncol. 8 (2007) 63–74.
[22] J.A. Loncaster, B.M. Carrington, J.R. Sykes, A.P. Jones, S.M. Todd, R. Cooper, D. L. Buckley, S.E. Davidson, J.P. Logue, R.D. Hunter, C.M.L. West, Prediction of radiotherapy outcome using dynamic contrast enhanced MRI of carcinoma of the cervix, Int. J. Radiat. Oncol. Biol. Phys. 54 (2002) 759–767.
[23] Sallinen H, Anttila M, Narvainen J, Koponen J, Hämäläinen K, Kholova I, Heikura T, Toivanen P, Kosma V-M, Heinonen S, Alitalo K, Ylä-Herttuala S. Antiangiogenic gene therapy with soluble VEGFR-1, -2, and -3 reduces the growth of solid human ovarian carcinoma in mice. Mol Ther 17(2):278–84.
[24] H.B. Salvesen, M.G. Gulluoglu, I. Stefansson, L.A. Akslen, Significance of CD 105 expression for tumour angiogenesis and prognosis in endometrial carcinomas, APMIS 111 (2003) 1011–1018.
[25] L.A. Solomon, A.R. Munkarah, V.L. Schimp, M.H. Arabi, R.T. Morris, H. Nassar, R. Ali-Fehmi, Maspin expression and localization impact on angiogenesis and prognosis in ovarian cancer, Gynecol. Oncol. 101 (2006) 385–389.
[26] S. Yang, H. Cheng, J. Cai, L. Cai, J. Zhang, Z. Wang, PlGF expression in pre-invasive and invasive lesions of uterine cervix is associated with angiogenesis and lymphangiogenesis, APMIS 117 (2009) 831–838.
[27] P. Carmeliet, R.K. Jain, Angiogenesis in cancer and other diseases, Nature 407 (2000) 249–257.
[28] A. Lindgren, M. Anttila, S. Rautiainen, O. Arponen, K. Hämäläinen, M. Könönen, R. Vanninen, H. Sallinen, Dynamic contrast-enhanced perfusion parameters in ovarian cancer: good accuracy in identifying high HIF-1α expression, PLoS One 22 (14) (2019) e0221340.
[29] S.B. Donaldson, G. Betts, S.C. Bonington, J.J. Homer, N.J. Slevin, L.E. Kershaw, H. Valentine, C.M.L. West, D.L. Buckley, Perfusion estimated with rapid dynamic contrast-enhanced magnetic resonance imaging correlates inversely with vascular endothelial growth factor expression and pimonidazole staining in head-and-neck cancer: a pilot study, Int. J. Radiat. Oncol. Biol. Phys. 81 (2011) 1176–1183.
[30] C.L. Mitchell, J.P.B. O'Connor, A. Jackson, G.J.M. Parker, C. Roberts, Y. Watson, S. Cheung, K. Davies, G.A. Buonaccorsi, A.R. Clamp, J. Hasan, L. Byrd, A. Backen, C. Dive, G.C. Jayson, Identification of early predictive imaging biomarkers and their relationship to serological angiogenic markers in patients with ovarian cancer with residual disease following cytotoxic therapy, Ann. Oncol. 21 (2010) 1982–2199.
[31] N. Di, W. Cheng, X. Jiang, X. Liu, J. Zhou, Q. Xie, Z. Chu, H. Chen, B. Wang, Can dynamic contrast-enhanced MRI evaluate VEGF expression in brain glioma? An MRI-guided stereotactic biopsy study, J. Neuroradiol. 46 (2019) 186–192.
[32] L. Ma, X. Xu, M. Zhang, S. Zheng, B. Zhang, W. Zhang, P. Wang, Dynamic contrast-enhanced MRI of gastric cancer: Correlations of the pharmacokinetic parameters with histological type, Lauren classification, and angiogenesis, Magn. Reson. Imaging 37 (2017) 27–32.
[33] K. Liu, P. Xie, W. Peng, Z. Zhou, Dynamic contrast-enhanced magnetic resonance imaging for pancreatic ductal adenocarcinoma at 3.0-T magnetic resonance: correlation with histopathology, J. Comput. Assist. Tomogr. 39 (2015) 13–18.
[34] V.C. Keil, B. Pintea, G.H. Gielen, K. Hittatiya, A. Datsi, M. Simon, R. Fimmers, H. H. Schild, D.R. Hadizadeh, Meningioma assessment: Kinetic parameters in dynamic contrast-enhanced MRI appear independent from microvascular anatomy and VEGF expression, J. Neuroradiol. 45 (2018) 242–248.
[35] I. Thomassin-Naggara, M. Bazot, E. Daraï, P. Callard, J. Thomassin, C.A. Cuenod, Epithelial ovarian tumors: value of dynamic contrast-enhanced MR imaging and correlation with tumor angiogenesis, Radiology 248 (2008) 148–159.
[36] W.W. Yao, H. Zhang, B. Ding, T. Fu, H. Jia, L. Pang, L. Song, W. Xu, Q. Song, K. Chen, Z. Pan, Rectal cancer: 3D dynamic contrast-enhanced MRI; correlation with microvascular density and clinicopathological features, Radiol. Medica. 116 (2011) 366–374.
[37] Kim SH, Lee HS, Kang BJ, Song BJoo, Kim H-B, Lee H, Jin M-S, Lee A. Dynamic contrast-enhanced MRI perfusion parameters as imaging biomarkers of angiogenesis. PLoS One 2016;11:e0168632.
[38] A. Oto, C. Yang, A. Kayhan, M. Tretiakova, T. Antic, C. Schmid-Tannwald, S. Eggener, G.S. Karczmar, W.M. Stadler, Diffusion-weighted and dynamic contrast-enhanced MRI of prostate cancer: correlation of quantitative MR parameters with Gleason score and tumor angiogenesis, Am. J. Roentgenol. 197 (2011) 1382–1390.
[39] I.S. Haldorsen, I. Stefansson, R. Grüner, J.A. Husby, I.J. Magnussen, H.M.J. Werner, Ø.O. Salvesen, L. Bjørge, J. Trovik, T. Taxt, L.A. Akslen, H.B. Salvesen, Increased microvascular proliferation is negatively correlated to tumour blood flow and is associated with unfavourable outcome in endometrial carcinomas, Br. J. Cancer 110 (2014) 107–114.
[40] V. Romeo, C. Cavaliere, M. Imbriaco, F. Verde, M. Petretta, M. Franzese, A. Stanzione, R. Cuocolo, M. Aiello, L. Basso, M. Amitrano, R. Lauria, A. Accurso, A. Brunetti, M. Salvatore, Tumor segmentation analysis at different post-contrast time points: a possible source of variability of quantitative DCE-MRI parameters in locally advanced breast cancer, Eur. J. Radiol. 126 (2020), 108907.
[41] X.M. Zhang, D. Yu, H.L. Zhang, Y. Dai, D. Bi, Z. Liu, M.R. Prince, C. Li, 3D dynamic contrast-enhanced MRI of rectal carcinoma at 3T: correlation with microvascular density and vascular endothelial growth factor markers of tumor angiogenesis, J. Magn. Reson. Imaging 27 (2008) 1309–1316.
[42] J.F.A. Jansen, D.L. Carlson, Y. Lu, H.E. Stambuk, A.L. Moreira, B. Singh, S.G. Patel, D.H. Kraus, R.J. Wong, A.R. Shaha, J.P. Shah, A. Shukla-Dave, Correlation of a priori DCE-MRI and (1)H-MRS data with molecular markers in neck nodal metastases: Initial analysis, Oral Oncol. 48 (2012) 717–722.
[43] Y.-E. Kim, J.S. Lim, J. Choi, D. Kim, S. Myoung, M.-J. Kim, K.W. Kim, Perfusion parameters of dynamic contrast-enhanced magnetic resonance imaging in patients with rectal cancer: Correlation with microvascular density and vascular endothelial growth factor expression, Korean J. Radiol. 14 (2013) 878–885.
[44] A. Surov, H.J. Meyer, M. Gawlitza, A.-K. Höhn, A. Boehm, T. Kahn, P. Stumpp, Correlations between DCE MRI and histopathological parameters in head and neck squamous cell carcinoma, Transl. Oncol. 10 (2017) 17–21.